Food and Chemical Toxicology 124 (2019) 400–410

Contents lists available at ScienceDirect

Food and Chemical Toxicology

journal homepage: www.elsevier.com/locate/foodchemtox

Cordycepin, isolated from medicinal fungus *Cordyceps sinensis*, enhances radiosensitivity of oral cancer associated with modulation of DNA damage repair

Nai-Wen Su[a,b], Shu-Hua Wu[c], Chih-Wen Chi[c], Tung-Hu Tsai[b,d,**], Yu-Jen Chen[b,c,e,f,g,*]

[a] Division of Medical Oncology and Hematology, Department of Internal Medicine, MacKay Memorial Hospital, Taipei, 11094, Taiwan
[b] Institute of Tradition Medicine, School of Medicine, National Yang-Ming University, Taipei, 11221, Taiwan
[c] Department of Medical Research, MacKay Memorial Hospital, Taipei, 25160, Taiwan
[d] Department of Chemical Engineering, National United University, Miaoli, 36063, Taiwan
[e] Department of Radiation Oncology, MacKay Memorial Hospital, Taipei, 25160, Taiwan
[f] Research Center for Chinese Medicine and Acupuncture, China Medical University, Taichung, 40402, Taiwan
[g] Department of Medical Research, China Medical University Hospital, Taichung, 40402, Taiwan

ARTICLE INFO

Keywords:
Cordycepin
Radiotherapy
Oral squamous cell carcinoma
Radiosensitivity
DNA damage response

ABSTRACT

Concurrent chemotherapy and radiotherapy (RT) is important for controlling oral squamous cell carcinoma (OSCC), which is often accompanied by significant acute and late toxicities. We investigated whether cordycepin, a small molecule extracted from *Cordyceps sinensis*, could enhance the radiosensitivity of oral cancer cells. Using colony formation assay, we demonstrated that cordycepin induces radiosensitizing effects on two OSCC cells. DNA histogram analysis showed that cordycepin combined with RT prolonged the RT-induced G2/M phase arrest. It protracted the duration of DNA double strand breaks, which was detected by immunofluorescent staining of phosphorylated histone H2AX (γ-H2AX). The underlying molecular mechanism might involve the downregulation of protein expression related to DNA damage repair, including phosphorylated ataxia-telangiectasia mutated (p-ATM) and phosphorylated checkpoint kinase 2. Reciprocal upregulation of phosphorylated checkpoint kinase 1 (Chk1) expression was noted, and the radiosensitizing effect of cordycepin could be further augmented by Chk1 mRNA knockdown, indicating a compensatory DNA repair machinery involving phosphorylation of Chk1. *In vivo*, the combination of cordycepin and RT exhibited greater growth inhibition on xenografts and stronger apoptosis induction than RT alone, without exacerbating major toxicities. In conclusion, cordycepin increased the radiosensitivity of OSCC cells, which is associated with the modulation of RT-induced DNA damage repair machinery.

1. Introduction

Head and neck squamous cell carcinoma (HNSCC) is a common cancer type worldwide with a yearly incidence of 600,000 cases, causing mortality in 50% of patients eventually (Ferlay et al., 2015). Combined multidisciplinary therapeutics is the corner-stone of treatments for the majority patients presenting with HNSCC at a locally advanced disease status (Argiris et al., 2008; Haddad and Shin, 2008). Among the treatment modalities, concurrent chemoradiotherapy (CCRT) can provide a definitive treatment for HNSCC; or it can be administered as the adjuvant therapy after major surgery (Bernier et al., 2004; Cooper et al., 2004; Gregoire et al., 2015). Currently, high-dose cisplatin is regarded as the gold standard radiosensitizer in CCRT worldwide (Forastiere et al., 2013). However, the addition of cisplatin to radiotherapy (RT) not only improves the disease control rate, but also significantly exacerbates acute and late side effects, including dermatitis, mucositis, xerostomia, neck fibrosis and myelopathy (Nguyen-Tan et al., 2014; Szturz et al., 2017). Unfortunately, there exists a recurrence rate of oral cancer even after management with standard CCRT (Iyer et al., 2015). Thus, development of more effective

Abbreviations: ATM, ataxia-telangiectasia mutated; ATR, ataxia-telangiectasia and Rad3 related; CCRT, concurrent chemoradiotherapy; Chk1, checkpoint kinase 1; Chk2, checkpoint kinase 2; DDR, DNA damage response; DNA-PKcs, DNA protein kinase catalytic subunit; DSB, double strand break; HR, homologous recombination; NHEJ, non-homologous end-joining; RT, radiotherapy; γ-H2AX, phosphorylated histone H2AX; SER, sensitizer enhancement ratio

* Corresponding author. Institute of Tradition Medicine, School of Medicine, National Yang-Ming, University, Taipei, 11221, Taiwan.
** Corresponding author. Institute of Tradition Medicine, School of Medicine, National Yang-Ming University, Taipei, 11221, Taiwan.
E-mail addresses: thtsai@ym.edu.tw (T.-H. Tsai), chenmdphd@gmail.com (Y.-J. Chen).

https://doi.org/10.1016/j.fct.2018.12.025
Received 30 October 2018; Received in revised form 8 December 2018; Accepted 17 December 2018
Available online 18 December 2018
0278-6915/

and better tolerated radiosensitizing agents without toxicity per se, especially from onotoxic natural products, is an urgent medical need (Bentzen et al., 2015; Ferris et al., 2016; Tang et al., 2018).

From the perspective of radiobiology, there are five principal factors (5Rs) that critically determine the cytotoxic effect of radiotherapy on cancer cells. They are as follows: repair of DNA damage, redistribution of cell cycle, repopulation, reoxygenation and intrinsic radiosensitivity (Harrington et al., 2007; Brown et al., 2014). Among these, DNA repair system and cell cycle regulation are investigated for radiosensitizers as known as new therapeutics to improve the radiotherapy efficacy. When ionizing radiation cause lethal DNA lesions such as double strand break (DSB), two major processes would be activated to maintain the genetic integrity (Pawlik and Keyomarsi, 2004). One is DNA repair machinery which correct and fix the DNA lesions. The other is cell cycle checkpoint pathway which halts the cell cycle progression to allow the cells repair the DNA damage in a prompt and accurate fashion (Mladenov et al., 2013). Many important regulatory proteins involve in this whole process of DNA damage response (DDR), such as ataxia-telangiectasia mutated (ATM) and checkpoint kinase 1(Chk1). These proteins might be suitable targets for drug development to enhance radiosensitivity (Morgan and Lawrence, 2015).

Cordyceps sinensis, a fungus that parasitizes the larvae of Lepidoptera, is a well-known and precious traditional Chinese medicine (Liu et al., 2015). For centuries of history, *C. sinensis* has been used extensively as a herbal medicinal remedy or as a healthy food to boost energy (Feng et al., 2017). Cordycepin, one of the important compounds extracted from *C. sinensis* possesses a variety of bioactivities (Tuli et al., 2013), has been characterized as an adenosine analogue. Many reports have demonstrated its anticancer activities on several cancer types, through inducing apoptosis or inhibiting metastasis (Chaicharoenaudomrung et al., 2018; Chou et al., 2014; Joo et al., 2017). Cordycepin was also shown to act synergistically with chemotherapy (Chen et al., 2013). In our previous study, metronomic dosing of cordycepin prolonged the survival of mice with oral cancer through inhibition of the epithelial mesenchymal transition (Su et al., 2017). We also found that cordycepin treatment arrests the G2/M phase of oral cancer cells, which provides a clue as to how cordycepin might enhance the radiosensitivity of cancer cells (Hofstetter et al., 2005). Although less reported, cordycepin also induces G2/M phase arrest and increases the radiosensitivity of other cancer types (Lee et al., 2009, 2010; Seong et al., 2016). In current study, we investigated the cytotoxic effects of cordycepin in combination with RT on the oral cancer cells both *in vitro* and *in vivo*. The results demonstrate that cordycepin could enhance the radiosensitivity through prolongation of the G2/M phase and regulation of DNA damage response.

2. Materials and methods

2.1. Materials and reagents

Cordycepin was obtained from Tokyo Chemical Industry (Kashiai, Japan). Mouse antibodies against Ku70 and Ku80 were purchased from BD Transduction Laboratory (San Jose, CA, USA) and β-Actin was purchased from Cell Signaling (Danvers, MA, USA). Rabbit antibodies against phosphorylated ATM (phosphor-ATM, Ser, 1981), phosphorylated ataxia-telangiectasia and Rad3 related (phosphor-ATR, Ser 428), phosphorylated checkpoint kinase 1 (phosphor-Chk1, Ser317), phosphorylated checkpoint kinase 2 (phosphor-Chk2, Thr68), RAD51, DNA protein kinase catalytic subunit (DNA-PKcs), cleaved caspase-3 (Asp75) and phosphorylated histone H2AX (Ser139) (<gamma>-H2AX) were all purchased from Cell Signaling (Danvers, MA, USA).

2.2. Cell lines and cell culture

Two oral squamous cell carcinoma (OSCC) cell lines were used in this study: an SAS cell line purchased from American Type Culture Collection (Manassas, VA, USA) and an OC-3 cell line that was kindly provided by Professor CJ Liu (Taipei, Taiwan). SAS cells were maintained in Dulbecco's Modified Eagle Medium (DMEM) supplemented with 10% v/v heat-inactivated fetal bovine serum (pH 7.4), 1% non-essential amino acid, 1% sodium pyruvate, and 1% streptomycin. OC-3 cells were cultured in DMEM supplemented with 10% v/v heat-inactivated fetal bovine serum (pH 7.4), 1% L-glutamine and 1% streptomycin. Both cell lines were incubated in a humidified atmosphere containing 95% air and 5% CO_2 at 37 °C. We passaged the cells every 3 days with Trypsin-EDTA-glucose solution (0.25% trypsin, 0.1% EDTA, and 0.05% glucose in Hanks' balanced salt solution) and maintained the cells in exponential growth.

2.3. Colony formation assay

The 2 OSCC cells were seeded onto the culture dishes at a concentration of 150 cells per dish. Cordycepin was added into the medium with the dose gradient of 0, 1, 10, 20 μM (for OC-3 cells, cordycepin was used up to concentration 50 μM) and maintained for 24 h. The cordycepin was washed out and the cells were then irradiated at various doses (0, 1, 2, 4Gy) administered in a single fraction using a 6 MeV electron beam generated by a linear accelerator (Clinac 18, Varian Associates, Inc, Palo Alto, CA, USA) at a dose rate of 2.4 Gy/min in a single fraction. Full electron equilibrium was ensured for each fraction by a parallel plate in a PR-60C ionization chamber (CAPINTEL, Inc, Ramsey, NY, USA). The cells were cultured for another 7 days and then stained with 3% crystal violet. The numbers of colonies containing more than 50 cells was counted. The surviving fraction was calculated as cells inoculated multiplied by plating efficiency. The sensitization enhancement ratio (SER) was calculated as the dose of radiation needed for RT alone divided by that required for cordycepin plus RT to yield a surviving fraction of 37%. D0 is the final slope of the survival curves fitted using a linear-quadratic model. SER was calculated by D0 without sensitizer/D0 with sensitizer.

2.4. Cell cycle analysis

SAS cells (1×10^5) were seeded on the culture plates and treated with cordycepin at concentrations of 0, 1, 10, 20 μM for 24 h. The cordycepin was washed out and replaced with culture medium, then immediately afterwards, the cells were irradiated with 0, 1, 2, 4 Gy. We collected the cells at 4, 8, 24 and 48 h after RT. Briefly, the collected cells were washed with PBS, and fixed in cold 70% ethanol. Before flow-cytometry analysis, the cells were re-washed and re-suspended in cold PBS, and incubated with10 mg/mL RNase and 1 mg/mL propidium iodide (PI) at 37 °C for 30 min in the dark. We used flow cytometry BD FACS Calibur™, BD Bioscience, San Jose, CA, USA) for cell cycle analysis. The cell cycle distribution (G0/G1, S, G2/M phases) of the cancer cells were determined by Cell Quest Software (version 2.01.2 Becton Dickinson, Franklin Lakes, NY, USA).

2.5. Immunofluorescence analysis of γH2AX

SAS cells were treated with 0 or 20 μM cordycepin for 24 h, followed by the replacement of the medium and RT at 0 or 4 Gy. The cells were harvested at 15 min, 1 h, 3, 4, 5 and 6 h after radiation exposure. Then we washed the cells with PBS, fixed in 4% paraformaldehyde for 15 min and permeabilized in 1% TritonX-100 in double distilled H_2O for 10 min. The cells were incubated with primary rabbit antihuman monoclonal antibody against γH2AX phosphorylated at serine 139 (1:200 dilution) and followed by secondary rhodamine red-conjugated goat antirabbit immunoglobulin G antibody (1:400 dilution; Jackson ImmunoResearch Laboratories, Inc., West Grove, PA, USA). Lastly, the cells were reacted with Hoechst 33342 (1:2000) (Sigma-Aldrich, Eugene, OR, USA) to stain the cell nuclei. The slides were fixed and observed by an Axiophot fluorescence microscope (Carl Zeiss Meditec

AG, Jena, Germany) and photographed by a digital camera system (Carl Zeiss AxioCam HRm, v.2.0, black and white version, Carl Zeiss Meditec AG).

2.6. Flow cytometric analysis of γH2AX

SAS cells were treated with cordycepin at concentrations of 0 and 20 μM for 24 h and the cordycepin-containing medium was washed and replaced. Immediately afterwards, the cells received RT at 0 and 4 Gy. The treated cells were then collected at 30 min, 1 h, 2, 6 and 24 h after RT. Each tube contained 3×10^5 cells and fixed with 4% paraformaldehyde. Before flow cytometric analysis, the cells were washed and resuspended in PBS and treated with 1% Triton-X for 10 min. Afterwards, the cells were reacted with γH2AX antibodies for 45 min and analyzed by flow cytometry. The γH2AX were measured using a BD FACS Calibur™(BD Bioscience, San Jose, CA, USA) and presented as the geometric means.

2.7. Western blot analysis

The SAS cells were treated with 0 or 20 μM cordycepin for 24 h and then subjected to RT at 0 or 4 Gy. We collected the cells at 1 and 6 h after RT and prepared the whole cell lysates. Forty micrograms of the protein extracts were used for the experiments. The membrane was blocked with 5% skim milk and reacted with primary antibodies against p-Chk1, p-Chk2, p-ATM, p-ATR, Ku70, Ku80, RAD51, DNA-PKcs, and β-actin at 4 °C overnight. Then the secondary goat antimouse antibody (Merck Millipore, Darmstadt, Germany) or a goat anti-rabbit antibody (Jackson ImmunoResearch Laboratories, Inc.) were added. The enhanced chemiluminescence system MultiGel-21 (TopBio Inc. Taipei, Taiwan) was used for final protein detection. The expression of β-actin was used as the internal control. The protein bands were measured and quantified by using image analysis software, Image- J.

2.8. Chk1 siRNA knockdown and colony formation assay

The SAS cells were plated on a 6-cm culture dish at a concentration of 1×10^5 cells/mL medium. The culture medium was changed to 5% fetal bovine serum without antibiotics 1 h before transfection. The Chk1 siRNA (120 pmol in 30 μL medium) was mixed with 8 μL of the transfection reagent (T-pro NTRII, T-Pro Biotechnology Inc., Taipei, Taiwan) for 15 min. Then the mixture was added into the culture dish and incubated for 24 h. After transfection, we performed western blot analysis of the Chk1 protein to verify the decreased protein expression. The siRNA used was Chk1 5′-GGC UUC GCA ACA GUA UUU CGG UAU A-3′, which was synthesized by Invitrogen (Carlsbad, CA, USA). In all the siRNA knockdown experiments, normal and non-specifically transfected (scrambled) SAS cells were used as negative controls. For the colony formation assay, we seeded 500 cells on the culture dish and performed the siRNA transfection procedure. Then we added 20 μM cordycepin and incubated the dish for 24 h, followed by RT using 0, 1, 2 and 4Gy treatments. The subsequent colony counting and survival fraction calculation were conducted in the same way as described in section 2.3.

2.9. Animals and in vivo experiments

Animal welfare was maintained according to the regulations of our institution's animal experiment committee (approval number: MMH-A-S-102-25). Six-to-eight- week-old BALB/c nude mice were bred and kept in an aseptic environment. We first injected oral cancer SAS cells (total 1×10^6 in 100 μL) subcutaneously over the right gluteal region in each mouse. Tumors were allowed to grow up to 0.5 cm^3. During this time, we randomly distributed the mice into 4 groups, consisting of the control group (PBS, phosphate buffered saline), RT group, cordycepin group and combination (RT + cordycepin) group. Both PBS and cordycepin at 50 μM were administered through intraperitoneally 5 days a week up to a maximum of 5 weeks. Tumors were irradiated using a 6 MeV electron beam generated by a linear accelerator (Clinac, 1800; Varian Associates, Inc, Palo Alto, CA, USA) at a dose rate of 2.4 Gy/min per fraction for 3 days in the first week of the experiment. The combination group received the same dose and schedule of RT and cordycepin as described above. The size of tumor growth and weight of the mice were measured and recorded thrice a week. Blood tests, consisting of white blood cell (WBC) counts, serum creatinine and serum alanine aminotransferase (ALT) were performed weekly. The mice were sacrificed at the end of 5 weeks of treatment. Tumor size was calculated by formula $(4\pi/3) \times (\text{width}/2)^2 \times (\text{length}/2)$.

2.10. Immunohistochemistry staining of cleaved caspase-3 in xenograft tumor

The formalin-fixed, paraffin-embedded excised tumors were sliced into 4-μm-thick tissue sections. The slides were treated with heat-induced antigen retrieval at 95 °C in sodium citrate buffer (10 mM, pH 6.0) for 30 min and then blocked by 3% hydrogen peroxide (H_2O_2) at 25 °C for another 30 min. Nonspecific reactions were blocked by BlockPRO™ Blocking Buffer (Visual Protein, Taipei, Taiwan) at room temperature for 30 min. Sections were reacted with primary antibody against cleaved Caspase-3(Casp-3) (1:200; Cell Signaling, Denver, MA, USA) overnight at 4 °C. This was followed by analysis using the VECTASTAIN abc Kit (Rabbit IgG) (PK-6101; Vector Laboratories, Peterborough, UK). Sections were stained with Liquid DAB + Substrate Chromogen System (DAKO, Carpinteria, CA, USA) and counterstained with hematoxylin. We consulted an oncological pathologist, who assisted in examining the staining pattern and judging the reactions. We observed cleaved Casp-3 positive cells through a light microscope and took 50 photographs of each tumor at a magnification of 400X (high power field, HPF). Then we counted the number of cleaved Casp-3 positive cells per HPF and used this as an index to quantify each treatment group.

2.11. Statistical analysis

All the experiments were performed at least thrice. Data were analyzed, and all the values are expressed as mean ± standard deviation (SD). The statistical analyses were performed with IBM SPSS statistics 20 (IBM Co., New York, NC, USA). One-way analysis of variance (ANOVA) was used to determine the statistical significance among groups. Student's T test was used for comparing two groups. A p-value of < 0.05 was considered statistically significant.

3. Results

3.1. Cordycepin enhanced radiosensitivity of OSCC cells

The colony formation assay showed that colony formation abilities decreased in both SAS and OC-3 cells when comparing the combined cordycepin plus RT to RT alone treatments. The SER was 1.719 for SAS cells at the cordycepin concentration of 20 μM (Fig. 1A). The SER was 1.406 for OC-3 cells at the cordycepin concentration of 50 μM (Fig. 1B).

3.2. Cordycepin, combined with radiotherapy, prolonged the G2/M phase

Cordycepin alone promotes G2/M phase arrest of SAS cells, as we have found in our previous study (Su et al., 2017). When we combined cordycepin (10 or 20 μM) with RT (4Gy), the proportion of cells arrested in G2/M phase 8 h after RT increased compared to that 4 h after RT. This increasing proportion of G2/M phase cells persisted and culminated at 24 h after RT (Fig. 2A). The proportion of G2/M phase cells was significantly higher with 20 μM cordycepin (71.09 ± 1.58%) than with 10 μM cordycepin (60.62 ± 0.29%) and the control group

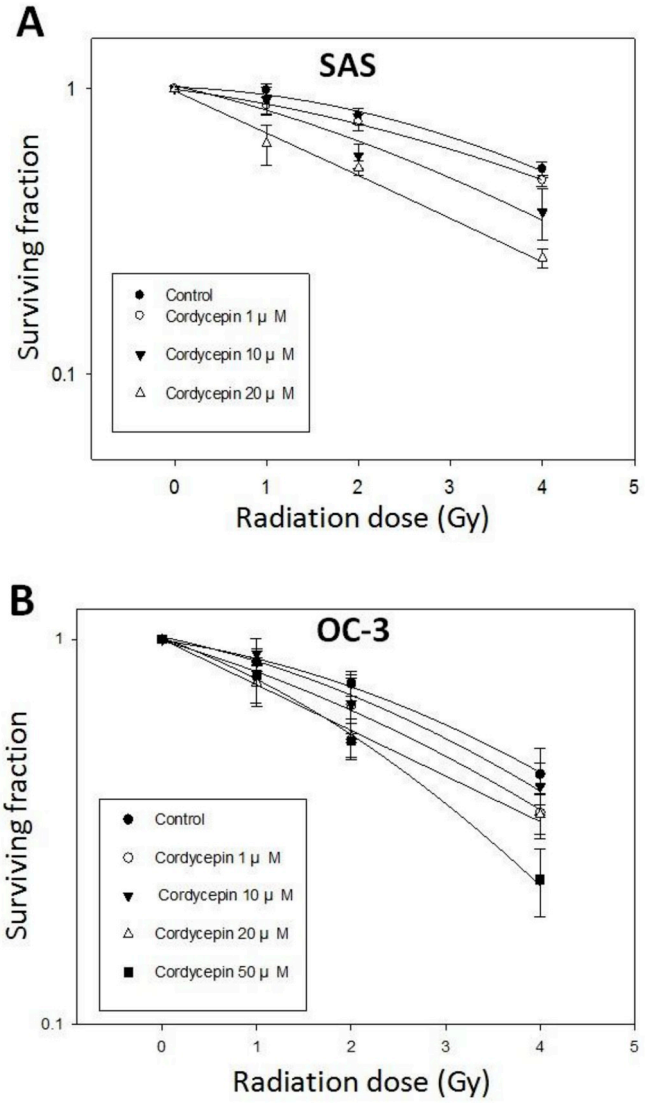

Fig. 1. Cordycepin enhanced the radiosensitivity of the OSCC cells. The 2 OSCC cells were plated onto the culture dishes and exposed to cordycepin at concentrations of 0, 1, 10, 20 and 50 μM for 24 h before RT. Then RT was administered at 0, 1, 2, 4 Gy, followed by the replacement with cordycepin-free culture medium. Colonies containing more than 50 cells were counted 7 days after RT. (A). SAS cells, (B) OC-3 cells. The experiments were repeated thrice.

(43.49 ± 2.42%) 24 h after 4 Gy RT treatment (Fig. 2B). We also observed that the proportion of G2/M phase cells returned to similarly low level (15–20%) in all treatment groups 48 h after RT.

3.3. Cordycepin protracted radiotherapy-induced DNA double strand breaks

Evaluating the presence of γ-H2AX, a biomarker of the double strand break, by immunofluorescence showed that RT induced a surge of γ-H2AX staining, which appeared as early as 15 min after RT, peaking at 1 h, and then subsiding gradually. SAS cells treated with combined cordycepin and RT exhibited significant longer and more intense γ-H2AX staining from 3 to 6 h when comparing to the RT alone group (Fig. 3A). Measuring the expression of γ-H2AX by flow cytometry (Fig. 3B) showed the expression levels peaking at 6 h for all the groups. However, a significantly higher γ-H2AX expression level was observed in the cordycepin plus RT group (geographic means ± S.E.; 19.56 ± 2.88), which was maintained until 24 h when comparing to other groups (RT group 10.77 ± 1.23; cordycepin group 9.66 ± 3.99; control group 7.65 ± 1.32) (Fig. 3C).

3.4. Cordycepin enhanced radiotherapy effects through the DNA damage repair machinery

We examined the 2 major upstream signaling pathways involving DDR, ATM-Chk2 and ATR-Chk1, and their downstream effector proteins. Western blotting showed that RT induced p-ATM and p-Chk2 expression. At 1 h after RT, the expression of p-ATM and p-Chk2 decreased in SAS cells pretreated by cordycepin when comparing to cells that received RT alone. The decreased p-Chk2 expression persisted for 6 h in the combined cordycepin and RT treatment group ($p < 0.05$). At the same time, we also found that either cordycepin treatment alone or combined with RT significantly increased p-Chk1 expression although the expression of p-ATR was relatively unchanged. There were no differences in the expression levels of the downstream DNA repair-associated proteins including, Ku70, Ku80, RAD51 and DNA PKcs (Fig. 4).

3.5. Knockdown of Chk1 sensitized the OSCC cells to combined radiation and cordycepin treatment

Chk1 protein knockdown through siRNA transfection and was verified by western blot analysis (Fig. 5A), followed by colony formation assay with 20 μM cordycepin and RT at 0, 1, 2, 4 Gy to all 3 cells. The results show that SAS cells with the Chk1 protein knockdown became sensitized to the combination treatment. The fraction of surviving SAS cells with Chk1 protein knockdown and administered with RT at 2Gy (SF2) was significantly suppressed at 46%, compared to 72% (normal SAS cells) and 68% (scrambled siRNA transfected SAS cells) (Fig. 5B).

3.6. Combined radiotherapy and cordycepin treatment inhibited OSCC xenograft tumor growth

Based on our previous study (Su et al., 2017), we adopted the same metronomic dosing schedule of cordycepin. Cordycepin was administered 5 days a week up to a maximum of 5 weeks at the concentration of 50 mg/kg whether alone or in combination with RT. We observed that the combination treatment delayed tumor growth significantly when compared to other groups (Fig. 6A). The mean tumor size at the end of the experiment was 1810.1 ± 409.1 cm^3 for the control group; 1365.8 ± 518.5 cm^3 for the RT group; 1387.0 ± 425.9 cm^3 for the cordycepin group and 897.2 ± 266.6 cm^3 for the combination group. We also concerned if the combination treatment would increase toxicities. There were no statistical differences in mice weights when comparing the cordycepin plus RT group to the other treatments (Fig. 6B). Moreover, we found no significant differences in white blood cell counts, alanine aminotransferase and serum creatinine levels among the 4 treatment groups (Fig. 6C, D and E).

3.7. Cordycepin plus irradiation promoted apoptosis of the OSCC tumor cells

Immunohistochemistry (IHC) staining of cleaved Casp-3 was performed on the formalin-fixed, paraffin-embedded xenograft tumor cells. Light mircoscopic observations showed more cleaved Casp-3 stained tumor cells in the combination treatment group compared to the other 3 groups (Fig. 7A–D). Counting of the cleaved Casp-3-stained cells among the 4 treatment groups based on 50 photographs of each tumor at 400× magnification (high power field, HPF) showed that there were significantly more cleaved Casp-3 positive tumor cells per HPF in the combination group (mean ± standard error, 6.53 ± 1.217) than the cordycepin (3.93 ± 0.665), RT (2.82 ± 0.348) and control groups (1.14 ± 0.181) (Fig. 7E).

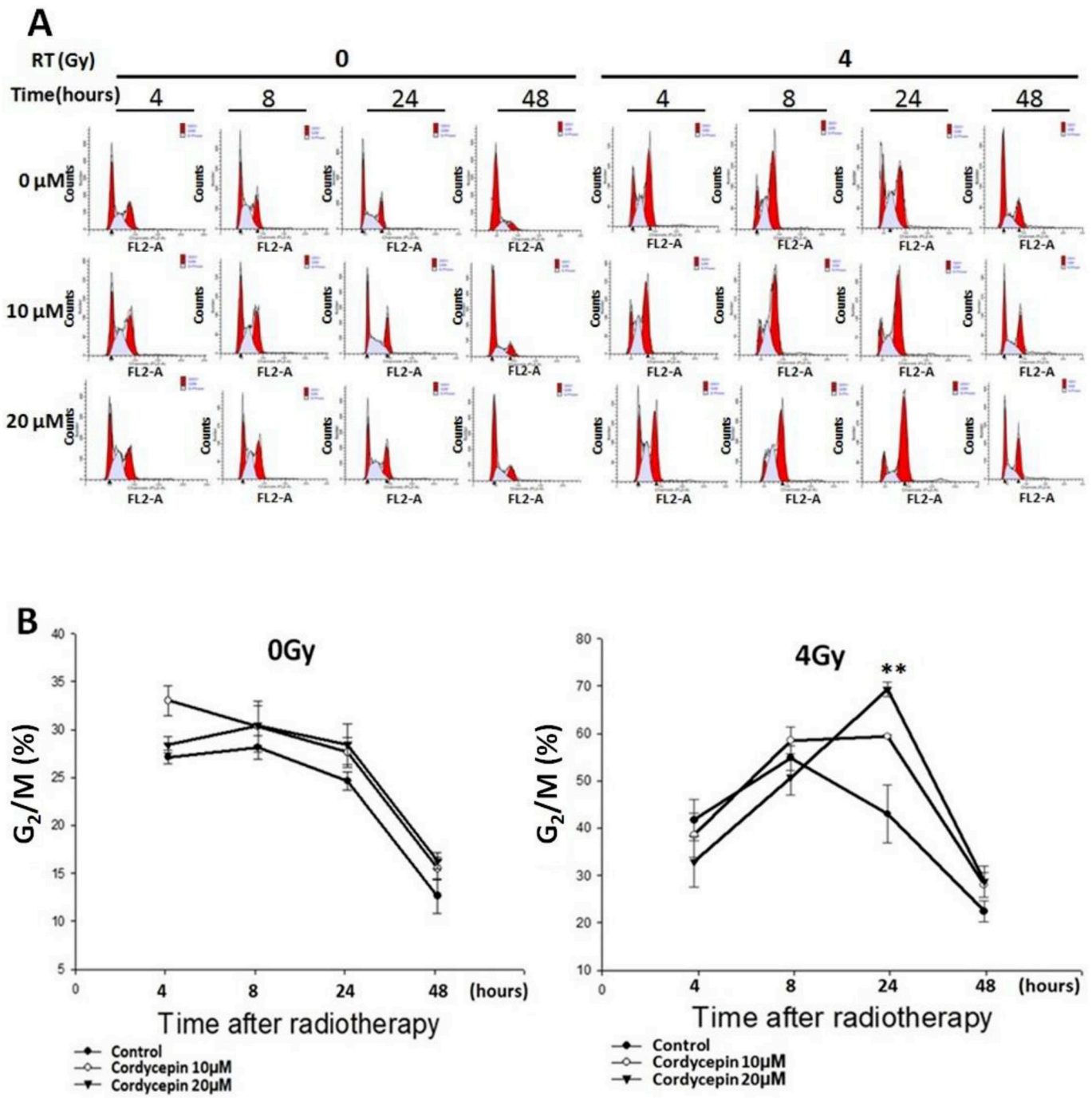

Fig. 2. Combined cordycepin and RT treatment prolonged G2/M phase arrest of OSCC cells. SAS cells were pretreated with 0, 10, 20 μM cordycepin for 24 h and then irradiated with 0 or 4Gy. We collected the cells at the indicated time points. (A) Cell cycle analyses were performed by using flow cytometry. (B) Radiotherapy at 4 Gy for cells treated with 20 μM cordycepin showed significantly more G2/M phase cells than the control group ($p < 0.05$), which culminated at 24 h after RT. The experiments were repeated 4 times. ** represents $p < 0.05$.

4. Discussion

Developments in radiation biology suggest that cells at G2/M phase are most vulnerable to radiotherapy (Pawlik and Keyomarsi, 2004). Since we have demonstrated that cordycepin alone could arrest OSCC cells at G2/M phase in a dose- and time-dependent manner (Su et al., 2017), then cordycepin might be synergistic to RT in cancer treatment. In the current study, cordycepin enhanced the radiation cytotoxicity to OSCC cells in colony formation assays and it also prolonged the G2/M phase arrest until 24 h after RT. On the other hand, RT is also known to induce the most lethal structural defect, DNA DSB (Vignard et al., 2013). Both immunofluorescence and flow-cytometry detection showed that combined cordycepin and RT treatment prolongs the expression of γ-H2AX, a hallmark of DNA DSB (Scully and Xie, 2013). DDR employs a complex machinery to help cells maintain genomic integrity by inhibiting cell cycle progression and promoting DNA repair (Magnander and Elmroth, 2012). If the DNA lesions are beyond repair, then the DDR could lead the cells into senescence or apoptosis. Among the DDR molecules, the most important DNA damage sensors and transducers are ATM-Chk2 and ATR-Chk1, which initiate two DNA repair pathway: homologous recombination (HR) or non-homologous end-joining (NHEJ) repair

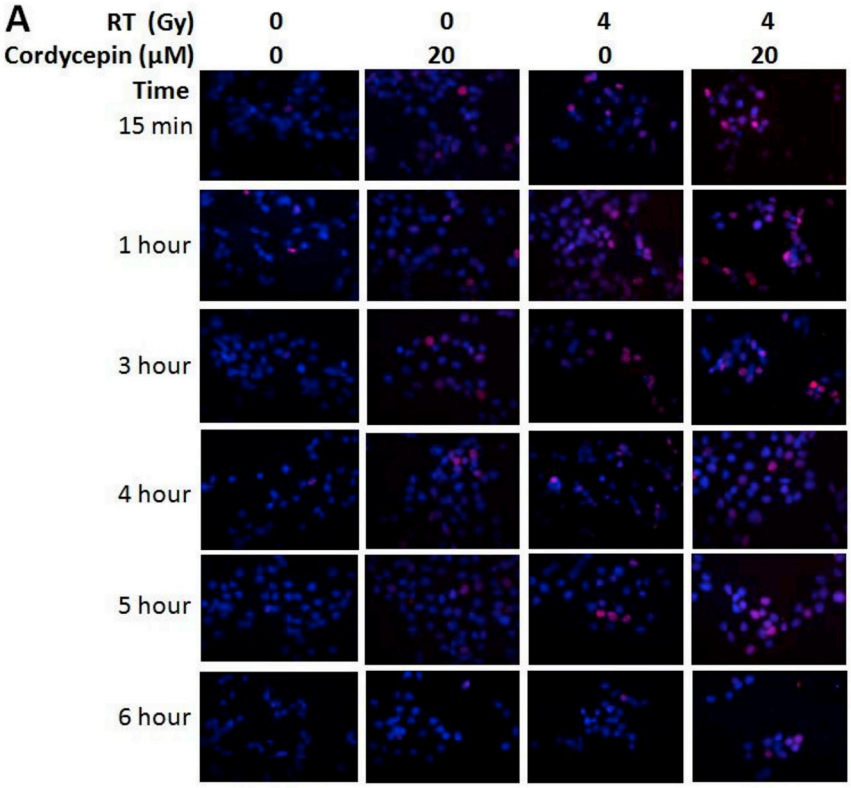

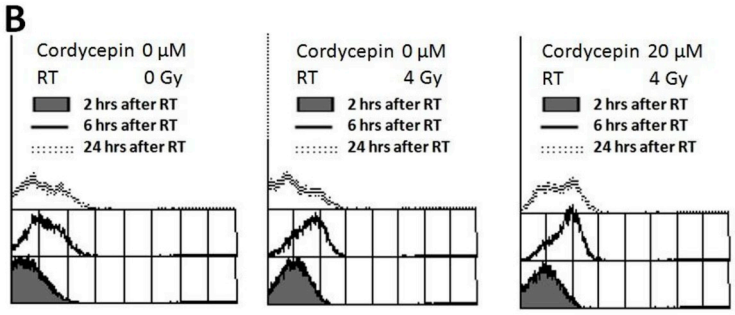

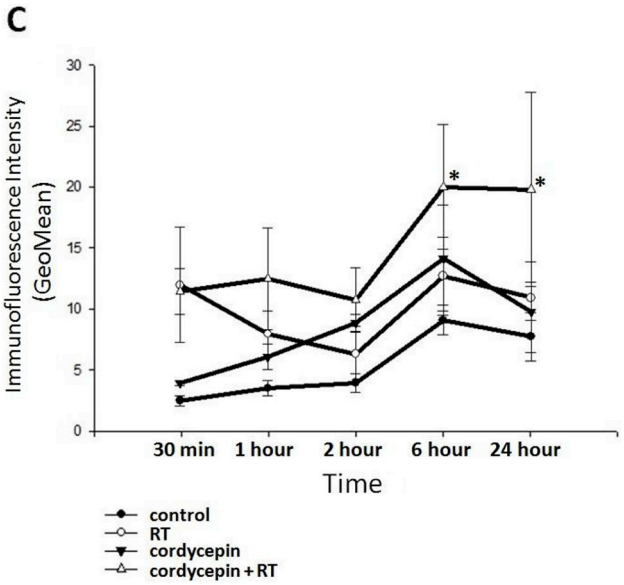

Fig. 3. Combination cordycepin and RT prolonged the presence of γ-H2AX, a biomarker of double strand breaks. (A) SAS cells were pretreated with 0 or 20 μM of cordycepin for 24 h and then followed by RT at 0 or 4 Gy. Then we collected cells at the indicated time points for immunofluorescence detection of γ-H2AX. (B) With the same dosing schedules of cordycepin and RT, we performed γ-H2AX analysis by flow cytometry. Representative flow cytometric detection is shown in Fig. 3B. (C) Quantitative comparisons showed that cells treated with cordycepin and RT had significantly more detectable γ-H2AX at 6 h after RT when comparing to the other groups. This level was maintained until 24 h after RT. The experiment was repeated 4 times. * represents $p < 0.05$.

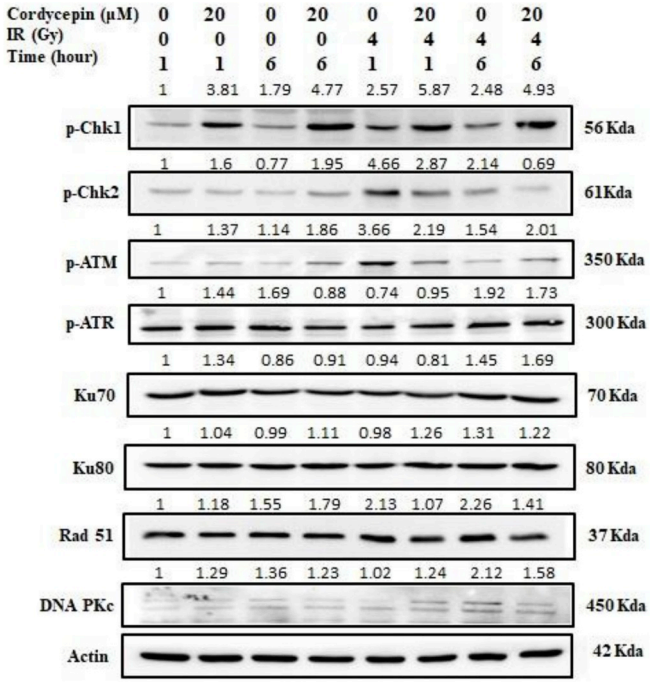

Fig. 4. Cordycepin enhanced radiation toxicity through the regulation of DNA damage response proteins. SAS cells were treated with 0 or 20 μM of cordycepin 24 h in advance, followed by RT at 0 or 4 Gy. The cells were collected at 1 or 6 h after RT treatment and total proteins were extracted and analyzed by immunoblotting. The name and molecular weight of each protein are noted in the figure. The numbers above each lane represent the mean folds of change in comparison to cells without cordycepin and RT treatment that were collected at 1 h after RT of other cells. The experiments were repeated thrice.

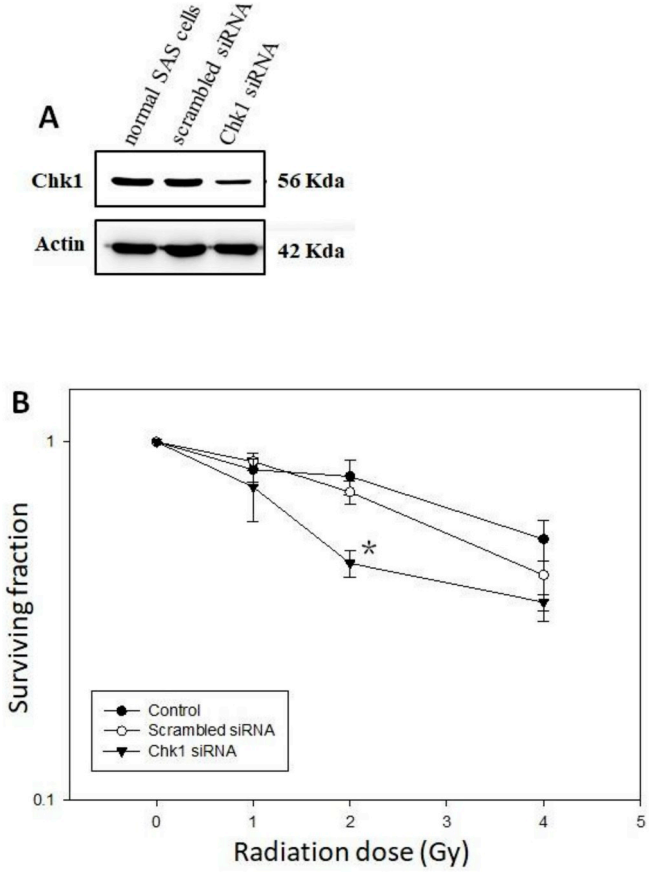

Fig. 5. Chk1 protein knockdown sensitizes the OSCC cells to cordycepin and RT treatment. (A) siRNA transfection for Chk1 protein knockdown was first performed and verified by western blot analysis. We used normal SAS cells and scrambled siRNA transfected SAS cells as negative controls. (B) Colony formation assay was performed by adding 20 μM of cordycepin and RT at doses of 0, 1, 2, 4 Gy to all 3 cells.
* represents $p < 0.05$. All the experiments were repeated thrice.

(Carrassa and Damia, 2017; Roos et al., 2016). The main repair system of cellular DNA DSB induced by RT is HR, which works in a more error-free fashion. Western blotting showed that cordycepin combined with RT decreased p-ATM and p-Chk2 expression when compared to RT treatment alone at 1 h after RT. The down-regulation of p-Chk2 persisted for 6 h after RT. This suppression of ATM-Chk2 signaling halts the HR DNA repair process, which might explain the radiosensitization effects of cordycepin. However, we also observed elevated p-Chk1 expression when cells were treated with cordycepin whether alone or combined with RT. We consider this result from two aspects. First, cordycepin itself, as an adenosine analogue, could cause stalling of the replication fork or DNA single-strand breakage (Nakamura et al., 2015). These damages mainly lead to the upregulation of ATR-Chk1 signaling to allow the DDR to proceed. Second, the suppression of ATM-Chk2 expression could ultimately upregulate the ATR-Chk1 as a self-protection mechanism and introduce redundancy between the DDR systems (Qiu et al., 2018; Sorensen et al., 2005; Wang et al., 2004). The two pathways, ATM-Chk2 and ATR-Chk1, are not simply acting in parallel. Laboratory evidences indicate that substantial crosstalk between the pathways exist intrinsically (Gatei et al., 2003; Hurley and Bunz, 2007; Jazayeri et al., 2006). For example, ATM-mediated DSB resection which leads to single stand DNA formation as an intermediate structure of DNA repair resulted in Chk1 recruitment and activation (Gottifredi and Prives, 2005; Jazayeri et al., 2006). On the other hand, activated Chk1 promotes DSB repair by recruiting HR factors, RAD51 and BRCA2, to the damage foci (Bahassi et al., 2008; Sorensen et al., 2005; Wang et al., 2004). Thus, we postulated that Chk1 upregulation could partly enhance DNA repair and protect the cancer cells from cell death in cells treated by cordycepin and RT. We subsequently knocked down Chk1 to verify if cordycepin-enhanced radiosensitivity could be further strengthened. The outcome showed that under the combined cordycepin and RT treatment, the Chk1 knockdown cells had inferior colony forming ability when comparing to the cells with normal Chk1 expression. Our results mimic the therapeutic concept of synthetic lethality which the cytotoxicity could be enhanced by inhibiting two different DNA repair systems (Chan and Giaccia, 2011; Kowk et al., 2016). Similar synergistic anticancer and radiosensitizing effects were demonstrated in another study when cancer cells have both ATM deficiency and Chk1 depletion (Palii et al., 2013). We are aware that a variety of therapeutics targeting ATR/Chk1 have been developed and tested in preclinical and clinical settings in combination with either RT or nucleotide analogues (Qiu et al., 2018). However, only one article in the literature review reported the radiosensitizing effect of cordycepin focusing on cervical cancer (Seong et al., 2016). In that study, cordycepin enhanced radiosensitivity through the modulation of G2/M phase regulatory proteins such as cyclin B, cdc2 and cdc25; and the effects were different in two cervical cancer cell lines. Indeed, cordycepin or agents possessing radiosensitizing effects frequently interact with cell cycle regulators and the DDR machinery. The underlying molecular mechanisms might be cancer-type or cell-type specific.

In our study, we validated the radiosensitization effects of cordycepin in an *in vivo* murine model. The combination treatment group had significantly delayed tumor growth when comparing to either cordycepin or RT alone. The effect involved tumor cell apoptosis and was highlighted by cleaved caspase-3 staining. The multiple modes of cell death might be induced by ionizing radiation such as apoptosis, mitotic

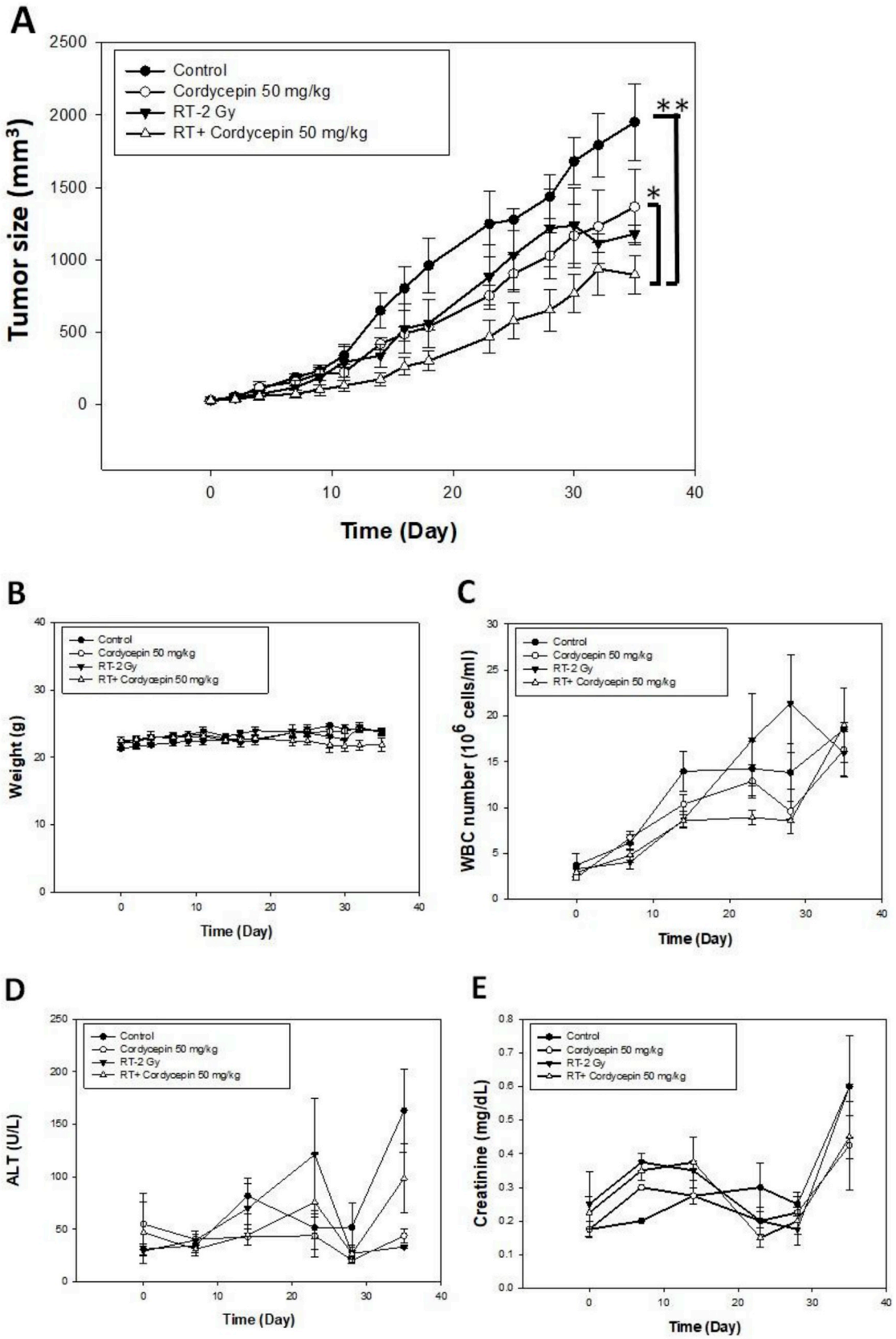

Fig. 6. Cordycepin in combination with RT delayed the OSCC tumor growth in the xenograft model. (A)The combined treatment with cordycepin plus RT delayed the growth of xenograft tumors when compared to cordycepin alone ($p < 0.05$), RT alone ($p < 0.05$) or the control group ($p < 0.01$). (B–E) For the toxicities evaluation, there were no statistical differences in mice weight, white blood cell counts, serum alanine aminotransferase and serum creatinine levels. * represents $p < 0.05$ and ** represents $p < 0.01$.

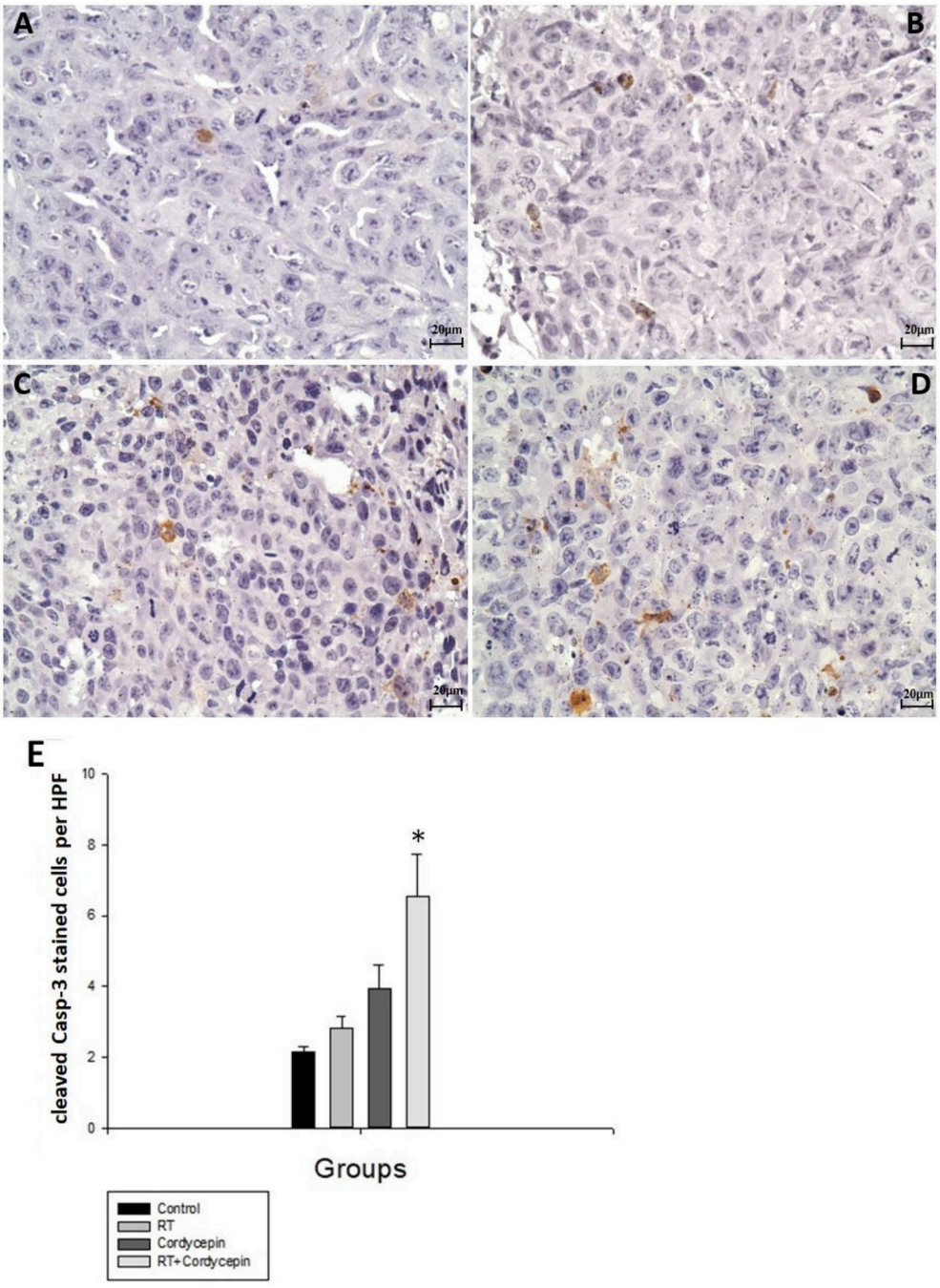

Fig. 7. Cordycepin plus radiotherapy increased apoptosis in OSCC tumor cells. Immunohistochemical staining of the cleaved Casp-3 was performed on xenograft tumor cells of each treatment group. More cleaved Casp-3 stained tumor cells were observed in the combination treatment group (A: control group; B: RT group; C: cordycepin group; D: cordycepin + RT). For quantitative comparison, we took 50 photographs of each tumor at the magnification 400X (high power field, HPF) and the cleaved Casp-3 stained tumor cells were counted. We compared the mean cleaved Casp-3 stained cells per HPF among the 4 groups. The tumors in combination group had significant more cleaved Casp-3 stained tumor cells in comparison to other treatment groups (Fig. 7E). * represents $p < 0.05$.

catastrophe, autophagy, necrosis and senescence. After carefully re-examination of our tumor specimen, the modes of cell death other than apoptosis are not evident by morphological observation. With our metronomic dosing schedule, we observed no additional toxicities in the combined cordycepin with RT treatment. From the perspective of developing novel therapeutics for HNSCC, there is a paramount advantage to enhance radiosensitivity while maintaining fewer toxicities. However, treatment resistance might be an unavoidable issue after repeated administration of cordycepin or nucleotide analogues. From our *in vitro* findings, a combination with inhibitors of ATM-Chk2 or ATR-Chk1 might further increase treatment efficacy and reduce the development of drug resistance.

In conclusion, our study demonstrated that cordycepin in combination with RT could prolong G2/M phase arrest and regulate DDR signaling. This radiosensitizing effect was also observed in the OSCC xenograft model.

5. Conclusion

Cordycepin, a natural occurring small molecule could enhance the radiosensitivity of oral cancer cells through prolonging G_2/M phase arrest and protracting double strand DNA breaks. The potential molecular mechanism might be related to the modulation of ATM-Chk2 and ATR-Chk1 pathway. The radiosensitivity induced by combining cordycepin and RT was demonstrated in a xenograft model by tumor growth delay with no excessive toxicities observed. This enforced radiosensitivity by cordycepin or its derivatives warrants further verification and clinical developments.

Conflicts of interest

The authors declare that there are no conflicts of interest.

Acknowledgments

This study was supported by Mackay Memorial Hospital (grant numbers MMH-E-107-13, MMH-E-106-13) and Ministry of Science and Technology, Taiwan (grant numbers MOST 106-2314-B-195-002-MY3, MOST 107-2623-E-195-001-NU)

Transparency document

Transparency document related to this article can be found online at https://doi.org/10.1016/j.fct.2018.12.025.

Appendix A. Supplementary data

Supplementary data to this article can be found online at https://doi.org/10.1016/j.fct.2018.12.025.

References

Argiris, A., Karamouzis, M.V., Raben, D., Ferris, R.L., 2008. Head and neck cancer. Lancet 371, 1695–1709. https://doi.org/10.1016/S0140-6736(08)60728-X.

Bahassi, E.M., Ovesen, J.L., Riesenberg, A.L., Bernstein, W.Z., Hasty, P.E., Stambrook, P.J., 2008. The checkpoint kinases Chk1 and Chk2 regulate the functional associations between hBRCA2 and Rad51 in response to DNA damage. Oncogene 27, 3977–3985. https://doi.org/10.1038/onc.2008.17.

Bentzen, J., Toustrup, K., Eriksen, J.G., Primdajl, H., Andersen, L.J., Overgaard, J., 2015. Locally advanced head and neck cancer treated with accelerated radiotherapy, the hypoxic modifier nimorazole and weekly cisplatin: results from the DAHANCA 18 phase II study. Acta Oncol. 54, 1001–1007. https://doi.org/10.3109/0284186X.2014.992547.

Bernier, J., Domenge, C., Ozsahin, M., Matuszewska, K., Lefebvre, J.L., Greiner, R.H., Giralt, J., Maingon, P., Rolland, F., Bolla, M., Cognetti, F., Bourhis, J., Kirkpatrick, A., van Glabbeke, M., 2004. European Organization for Research and Treatment of Cancer Trial 22931, Postoperative irradiation with or without concomitant chemotherapy for locally advanced head and neck cancer. N. Engl. J. Med. 350, 1945–1952.

Brown, J.M., Carlson, D.J., Brenner, D.J., 2014. The tumor radiobiology of SRS and SBRT: are more than the 5 Rs involved ? Int. J. Radiat. Oncol. Biol. Phys. 88, 254–262. https://dx.doi.org/10.1016/j.ijrobp.2013.07.022.

Carrassa, L., Damia, G., 2017. DNA damage response inhibitors: mechanisms and potential applications in cancer therapy. Cancer Treat Rev. 60, 139–151. https://doi.org/10.1016/j.ctrv.2017.08.013.

Chaicharoenaudomrung, N., Jaroonwitchawan, T., Noisa, P., 2018. Cordycepin induces apoptosis cell death of human brain cancer through modulation of autophagy. Toxicol. Vitro 46, 113–121. https://doi.org/10.1016/j.tiv.2017.10.002.

Chan, D.A., Giaccia, A.J., 2011. Harnessing synthetic lethal interaction in anticancer drug discovery. Nat. Rev. Drug Discov. 10, 351–364. https://doi.org/10.1038/nrd3374.

Chen, Y.H., Wang, J.Y., Pan, B.S., Mu, Y.F., Lain, M.S., So, E.C., Wong, T.S., Huang, B.M., 2013. Cordycepin enhances cisplatin apoptotic effect through caspase/MAPK pathways in human head and neck tumor cell. Oncol. Targets Ther. 6, 983–998. https://doi.org/10.2147/OTT.S45322.

Chou, S.M., Lai, W.J., Hong, T.W., Lai, J.Y., Tsai, S.H., Chen, Y.H., Yu, S., Kao, C.H., Chu, R., Ding, S.T., Li, T.K., Shen, T.L., 2014. Synergistic property of cordycepin in cultivated Cordyceps militaris-mediated apoptosis in human leukemia cells. Phytomedicine 21, 1516–1524. https://doi.org/10.1016/j.phymed.2014.07.014.

Cooper, J.S., Pajak, T.F., Forastiere, A.A., Jacobs, J., Campbell, B.H., Saxman, S.B., Kish, J.A., Lim, H.E., Cmelak, A.J., Rotman, M., Machtay, M., Ensley, J.F., Chao, K.S., Schultz, C.J., Lee, N., Fu, K.K., Radiation Therapy Oncology Group 9501/Intergroup, 2004. Postoperative concurrent radiotherapy and chemotherapy for high-risk squamous-cell carcinoma of the head and neck. N. Engl. J. Med. 350, 1937–1944.

Feng, K., Wang, L., Liao, D., Lu, X., Hu, D., Liang, X., Zhao, J., Mo, Z., Li, S., 2017. Potential molecular mechanisms for fruiting body formation of Cordyceps illustrated in the case of *Cordyceps sinensis*. Mycology 8, 231–258. http://doi.org/10.1080/21501203.2017.1365314.

Ferlay, J., Soerjomataram, I., Dikshit, R., Eser, S., Mathers, C., Rebelo, M., Parkin, D.M., Forman, D., Bray, F., 2015. Cancer incidence and mortaily worldwide: sources, methods and major patterns in GLOBOCAN 2012. Int. J. Canc. 136, E359–E386. https://doi.org/10.1002/ijc.29210.

Ferris, R.L., Geiger, J.L., Trivedi, S., Schmitt, N.C., Heron, D.E., Johnson, J.T., Kim, S., Duvvuri, U., Clump, D.A., Bauman, J.E., Ohr, J.P., Gooding, W.E., Argiris, A., 2016. Phase II trial of postoperative radiotherapy with concurrent cisplatin plus panitumumab in patients with high-risk, resected head and neck cancer. Ann. Oncol. 27, 2257–2262. https://doi.org/10.1093/annonc/mdw428.

Forastiere, A.A., Zhang, Q., Weber, M.H., Goepfert, H., Pajak, T.F., Morrison, W., Glisson, B., Trotti, A., Ridge, J.A., Thorstad, W., Wagner, H., Ensley, J.F., Cooper, J.S., 2013. Long-term results of RTOG 91-11: a comparison of three nonsurgical treatment strategies to preserve the larynx in patients with locally advanced larynx cancer. J. Clin. Oncol. 31, 845–852. https://doi.org/10.1200/JCO.2012.43.6097.

Gatei, M., Sloper, K., Sorensen, C., Syljuasen, R., Falck, J., Hobson, K., Savage, K., Lukas, J., Zhou, B.B., Bartek, J., Khanna, K.K., 2003. Ataxia-telangiectasia-mutated (ATM) and NBS1-dependent phosphorylation of Chk1 on Ser-317 in response to ionizing radiation. J. Biol. Chem. 278, 14806–14811.

Gottifredi, V., Prives, C., 2005. The S phase checkpoint: when the crowd meets at the fork. Semin. Cell Dev. Biol. 16, 355–368.

Gregoire, V., Langendijk, J.A., Nuyts, S., 2015. Advances in radiotherapy for head and neck cancer. J. Clin. Oncol. 33, 3277–3284. https://doi.org/10.1200/JCO.2015.61.2994.

Haddad, R.I., Shin, D.M., 2008. Recent advances in head and neck cancer. N. Engl. J. Med. 359, 1143–1154. https://doi.org/10.1056/NEJMra0707975.

Harrington, K., Hankowska, P., Hingorani, M., 2007. Molecular biology for thr radiation oncologist: the 5Rs of radiobiology meet the hallmarks of cancer. Clin. Oncol. 19, 561–571. https://doi.org/10.1016/j.clon.2007.04.009.

Hofstetter, B., Vuong, V., Broggini-Tenzer, A., Bodis, S., Ciernik, I.F., Fabbro, D., Wartmann, M., Folkers, G., Pruschy, M., 2005. Patupilone acts as radiosensitizing agent in multidrug-resistant cancer cells *in vitro* and *in vivo*. Clin. Canc. Res. 11, 1588–1596.

Hurley, P.J., Bunz, F., 2007. ATM and ATR, components of an integrated circuit. Cell Cycle 6, 414–417.

Iyer, N.G., Tan, D.S., Tan, V.K., Wang, W., Hwang, J., Tan, N.C., Sivanandan, R., Tan, H.K., Lim, W.T., Ang, M.K., Wee, J., Soo, K.C., Tan, E.H., 2015. Randomized trial comparing surgery and adjuvant radiotherapy versus concurrent chemoradiotherapy in patients with advanced, nonmetastatic squamous cell carcinoma of the head and neck: 10-year update and subset analysis. Cancer 121, 1599–1607. https://doi.org/10.1002/cncr.29251.

Jazayeri, A., Falck, J., Lukas, C., Bartek, J., Smith, G.C., Lukas, J., Jackson, S.P., 2006. ATM- and cell cycle-dependent regulation of ATR in response to DNA double-strand break. Nat. Cell Biol. 8, 37–45.

Joo, J.C., Hwang, J.H., Jo, E., Kim, Y.R., Kim, D.J., Lee, K.B., Park, S.J., Jang, I.S., 2017. Cordycepin induces apoptosis by caveolin-1-mediated JNK regulation of Foxo3a in human lung adenocarcinoma. Oncotarget 8, 12211–12224. https://doi.org/10.18632/oncotarget.14661.

Kwok, M., Davies, N., Agathanggelou, A., Smith, E., Oldreive, C., Petermann, E., Stewart, G., Brown, J., Lau, A., Pratt, G., Parry, H., Taylor, M., Moss, P., Hillmen, P., Stankovic, T., 2016. ATR inhibition induces synthetic lethality and overcomes chemoresistance in TP53- or ATM-defective chronic lymphocytic leukemia cells. Blood 127, 582–595. https://doi.org/10.1182/blood-2015-05-644872.

Lee, S.J., Kim, S.K., Choi, W.S., Kim, W.J., Moon, S.K., 2009. Cordycepin causes p21WAF1-mediated G2/M cell-cycle arrest by regulating c-Jun N-terminal kinase activation in human bladder cancer cells. Arch. Biochem. Biophys. 490, 103–109. https://doi.org/10.1016/j.abb.2009.09.001.

Lee, S.J., Moon, G.S., Jung, K.H., Kim, W.L., Moon, S.K., 2010. C-Jun N-terminal kinase 1 is required for cordycepin-mediated induction of G2/M cell-cycle arrest via p21WAF1 expression in human colon cancer cells. Food Chem. Toxicol. 48, 277–283. https://doi.org/10.1016/j.fct.2009.09.042.

Liu, Y., Wang, J., Wang, W., Zhang, H., Zhang, X., Han, C., 2015. The chemical constituents and pharmacological actions of Cordyceps sinensis. Evid. Based Complement. Alternat. Med. 5757063. 2015. https://doi.org/10.1155/2015/575063.

Magnander, K., Elmroth, K., 2012. Biological consequences of formation and repair of complex DNA damage. Cancer Lett. 327, 90–96. https://doi.org/10.1016/j.canlet.2012.02.013.

Mladenov, E., Magin, S., Soni, A., Iliakis, G., 2013. DNA double-strand break repair as determinant of cellular radiosensitivity to killing and target in radiation therapy. Front. Oncol. 3, 113. https://doi.org/10.3389/fonc.2013.00113.

Morgan, M.A., Lawrence, T.S., 2015. Molecular pathways: overcoming radiation resistance by targeting DNA damage response pathways. Clin. Canc. Res. 21, 2898–2904. https://doi.org/10.1158/1078-0432.CCR-13-3229.

Nakamura, K., Shinosuka, K., Yoshikawa, N., 2015. Anticancer and antimetastatic effects of cordycepin, an active component of Cordycepin sinensis. J. Pharmacol. Sci. 127, 53–56. https://doi.org/10.1016/j.jphs.2014.09.001.

Nguyen-Tan, P.S., Zhang, Q., Ang, K.K., Weber, R.S., Rosenthal, D.I., Soulieres, D., Kim, H., Silverman, C., Raben, A., Galloway, T.J., Fortin, A., Gore, E., Westra, W.H., Chung, C.H., Jordan, R.C., Gillison, M.L., List, M., Le, Q.T., 2014. Randomized phase III trialto test accelerated versus standard fractionation in combination with concurrent cisplatin for head and neck carcinomas in the Radiation Therapy Oncology Group 0129 trial: long-term report of efficacy and toxicity. J. Clin. Oncol. 32, 3858–3866. https://doi.org/10.1200/JCO.2014.55.3925.

Palii, S.S., Cui, Y., Innes, C.L., Paules, R.S., 2013. Dissecting cellular responses to irradiation via targeted disruptions of the ATM-CHK1-PP2A circuit. Cell Cycle 12, 1105–1118. https://doi.org/10.4161/cc.24127.

Pawlik, T.M., Keyomarsi, K., 2004. Role of cell cycle in mediating sensitivity to radiotherapy. Int. J. Radiat. Oncol. Biol. Phys. 48, 928–942.

Qiu, Z., Oleinick, N.L., Zhang, J., 2018. ATR/CHK1 inhibitors and cancer therapy. Radiother. Oncol. 126, 450–464. https://doi.org/10.1016/j.radonc.2017.09.043.

Roos, W.P., Thomas, A.D., Kaina, B., 2016. DNA damage and the balance between survival and death in cancer biology. Nat. Rev. Canc. 16, 20–33. https://doi.org/10.1038/nrc.2015.2.

Scully, R., Xie, A., 2013. Double strand break repair functions of histone H2AX. Mutat. Res. 750, 5–14. https://doi.org/10.1016/j.mrfmmm.2013.07.007.

Seong, D.B., Hong, S., Muthusami, S., Kim, W.D., Yu, J.R., Park, W.Y., 2016. Cordycepin increases radiosensitivity in cervical cancer cells by overriding or prolonging radiation-induced G2/M arrest. Eur. J. Pharmacol. 771, 77–83. https://doi.org/10.1016/j.ejphar.2015.12.022.

Sorensen, C.S., Hansen, L.T., Diegielewski, J., Syljuasen, R.G., Lundin, C., Bartek, J., Helleday, T., 2005. The cell-cycle checkpoint kinase Chk1 is required for mammalian homologous recombination repair. Nat. Cell Biol. 7, 195–201.

Su, N.W., Wu, S.H., Chi, C.W., Liu, C.J., Tsai, T.H., Chen, Y.J., 2017. Metronomic Cordycepin therapy prolongs survival of oral cancer-bearing mice and inhibits epithelial-mesenchymal transition. Molecules 22 Pii:E629. https://doi.org/10.3390/molecules22040629.

Szturz, P., Wouters, K., Kiyota, N., Prabhash, K., Noronha, V., Castro, A., Licitra, L., Adelstein, D., Vermorken, J.B., 2017. Weekly low-dose versus three-weekly high-dose cisplatin for concurrent chemoradiation in locoregionally advanced non-nasopharyngeal head and neck cancer: a systemic review and meta-analysis of aggregate data. Oncol. 22, 1056–1066. https://doi.org/10.1634/theoncologist.2017-0015.

Tang, L.Q., Chen, D.P., Guo, L., Mo, H.Y., Guo, S.S., Qi, B., Tang, Q.N., Wang, P., Li, X.Y., Li, J.B., Liu, Q., Gao, Y.H., Xie, F.Y., Liu, L.T., Li, Y., Liu, S.L., Xie, H.J., Liang, Y.J., Sun, X.S., Yan, J.J., Wu, Y.S., Luo, D.H., Huang, P.Y., Xiang, Y.Q., Sun, R., Chen, M.Y., Lv, X., Wang, L., Xia, W.X., Zhao, C., Cao, K.J., Qian, C.N., Guo, X., Hong, M.H., Nie, Z.Q., Chen, Q.Y., Mai, H.Q., 2018. Concurrent chemoradiotherapy with nedaplatin versus cisplatin in phase II-IVB nasopharyngeal carcinoma: an open-label, non-inferiority, randomized phase 3 trial. Lancet Oncol. 19, 461–473. https://doi.org/10.1016/S1470-2045(18)30104-9.

Tuli, H.S., Sharma, A.K., Sandhu, S.S., Kashyap, D., 2013. Cordycepin: a bioactive metabolite with therapeutic potential. Life Sci. 93, 863–869. https://doi.org/10.1016/j.lfs.2013.09.030.

Vignard, J., Mirey, G., Salles, B., 2013. Ionizing-radiation induced DNA double-strand breaks: a direct and indirect lighting up. Radiother. Oncol. 108, 362–369. https://doi.org/10.1016/j.radonc.2013.06.013.

Wang, H., Wang, H., Powell, S.N., Iliakis, G., Wang, Y., 2004. ATR affecting cell radiosensitivity is dependent on homologous recombination repair but independent of nonhomologous end joining. Cancer Res. 64, 7139–7143.